CAMBRIDGE UNIVERSITY

FIBRE-OPTIC SENSORS USING ADIABATICALLY TAPERED SINGLE-MODE FIBRES

A DISSERTATION SUBMITTED TO
THE FACULTY OF THE DIVISION OF ENGINEERING

IN CANDIDACY FOR THE DEGREE OF
CERTIFICATE OF POSTGRADUATE STUDY IN ENGINEERING

DEPARTMENT OF ELECTRICAL ENGINEERING

BY
ZOE M. HALE

CAMBRIDGE, UNITED KINGDOM
MAY 1992

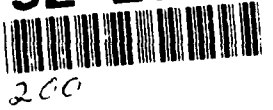

REPORT DOCUMENTATION PAGE

Form Approved
OMB No 0704-0188

1. AGENCY USE ONLY (Leave blank)	2. REPORT DATE	3. REPORT TYPE AND DATES COVERED
	May 1992	THESIS/DISSERTATION

4. TITLE AND SUBTITLE
Fibre-Optic Sensors Using Adiabatically Tapered Single-Mode Fibres

5. FUNDING NUMBERS

6. AUTHOR(S)
Zoe M. Hale, Captain

7. PERFORMING ORGANIZATION NAME(S) AND ADDRESS(ES)
AFIT Student Attending: Cambridge University

8. PERFORMING ORGANIZATION REPORT NUMBER
AFIT/CI/CIA- 92-047

9. SPONSORING/MONITORING AGENCY NAME(S) AND ADDRESS(ES)
AFIT/CI
Wright-Patterson AFB OH 45433-6583

10. SPONSORING/MONITORING AGENCY REPORT NUMBER

11. SUPPLEMENTARY NOTES

12a. DISTRIBUTION/AVAILABILITY STATEMENT
Approved for Public Release IAW 190-1
Distributed Unlimited
ERNEST A. HAYGOOD, Captain, USAF
Executive Officer

12b. DISTRIBUTION CODE

13. ABSTRACT (Maximum 200 words)

14. SUBJECT TERMS

15. NUMBER OF PAGES
40

16. PRICE CODE

17. SECURITY CLASSIFICATION OF REPORT	18. SECURITY CLASSIFICATION OF THIS PAGE	19. SECURITY CLASSIFICATION OF ABSTRACT	20. LIMITATION OF ABSTRACT

Abstract

A tapered single-mode fibre optic device was investigated for use as an intrinsic pH sensor. The sensing process is based on the detection of evanescent-wave excited fluorescence energy from an indicator dye circulating the taper. Appropriate selection of dye and taper parameters have allowed the sensor to perform well in harsh chemical environments, with near-real-time response. Future work could include immobilisation schemes for the indicator as well as other sensor types, such as pCa. Further optical properties of the tapered fibre will also be investigated.

TABLE OF CONTENTS

LIST OF ILLUSTRATIONS

1.0 Introduction

In this first year, I have examined the suitability of adiabatically single mode tapered fibres for sensor applications. To do so, I reviewed recent work on fibre optic sensors and chose to design an elementary pH sensor. Further, examining the characteristics of the tapered fibre as a waveguide led me to undertake efforts to optimise the use of the evanescent field. I accomplished this by choosing an appropriate indicator, excitation wavelength and external environment for the taper. I present here a summary of these efforts, including performance data from the sensor and a proposal for future work. For convenience of the reader, a glossary of the more chemistry-specific terms is found in Appendix I.

2.0 Discussion of the Literature

2.1 Fibre optic sensors:

Optical fibres have been explored extensively for their potential use as sensors. As better methods of exploiting and interpreting optical information arise, the situations in which fibres could be employed increase. Before we look at the potential applicability of the adiabatically tapered single-mode optical fibre for sensing, it is necessary to examine the requirements for acceptable sensors. Various descriptions of "good fibre sensors" differ, but several characteristics remain at the forefront of most discussions. Sensors in general need to have sensitivity in the range of interest as well as selectivity for the analyte. It is usually desirable for them to have a broad dynamic range and to perform reversibly. Sensors should be robust, reliable, and responsive, as well as not requiring frequent calibration. They should be above all inert to whatever media is sampled. Other sensor characteristics that are often considered desirable are small size, low cost and the capability to operate autonomously. [1]

To decide if the tapered fibre will fit some or all of these criteria, we first examine the fibre and its behaviour. An essential component of any form of chemical analysis using optical fibres is the optical fibre itself. This consists of a light-guiding core, usually a silica-based glass, surrounded by an optically rarer cladding. [2] It is this cladding that can be used as the basis for interaction with the analyte.

Several methods of interacting with the external analyte exist. Chemical dopants may be placed in polymer-based optical cladding materials to enhance the dependence of fibre transmission loss on the chemical composition of this surrounding environment. Another approach uses the inverse process: optical energy generated by fluorescent dye molecules in the cladding is coupled into the core by means of the evanescent fields of the guided mode(s). These sensors differ from fiber optic sensors based on direct evanescent-wave spectroscopy in that active substances having optical properties that depend on their chemical environment are made an integral part of the waveguide structure. [3]

Once the method of interaction has been established, the configuration of the sensor itself must be decided upon. Fibre optic sensors for both physical and chemical parameters can be divided into the following two types: (i) extrinsic sensors, where the optical fibre merely acts as a light-guiding link between the measurement point and the interrogating and display electronics and (ii) intrinsic sensors, where the fibre, probably in some modified form, is the sensing transducer. [4] Although typically more difficult to construct, intrinsic sensors are likely to be simple in terms of required components and thereby more suitable for meeting some of our requirements for "good" sensors.

All intrinsic fibre sensors are based on the modification of some optical property of the fibre by the analyte. By immobilising indicator dyes in the cladding, changes can be induced in the loss spectrum by analytes that have no native optical absorbance in the spectral range accessible to standard optical fibres. Such "active coating" sensors often provide much higher sensitivity than those based on direct spectroscopic detection of the

analyte. [5] Because the light in the fibre remains guided, interaction with the analyte (or an immobilised analyte-sensitive reagent) can only occur in or near, via evanescent wave interaction, the waveguide. Further, the ease of mass transport into the sensitive region will be dependent on the size and number of access-ways to the waveguiding region [6]. The tapered fibre provides both increased access and a larger surface area for dye immobilisation.

2.2 Construction of Sensors:

The ideal intrinsic sensor would utilise a scheme in which the evanescent wave was capable of interacting with an external analyte over a large surface area. The area available for interaction depends greatly on the method of immobilising the interactive reagent onto the waveguide. A fluorescent species just beyond the interface of cladding and external analyte can be excited by the evanescent wave interaction and the luminescent photons can couple back into the waveguide by the reverse effect. [7] Using this general technique, the change in transmission that occurs in the presence of the analyte can be more than ten orders of magnitude greater than the change in transmission due to simple optical absorbance of the analyte itself [8]. Several methods have been explored in order to bind the sensitive reagent to the waveguide.

Various solid supports such as glass, cellulose, polyacrylamide and polystyrene have been used for immobilisation. Their surfaces are readily endowed with amino groups to which an indicator can be limited. Glass is characterised by rigidity, transparency and resistance to bacteria. Cellulose is a much less rigid support, but offers other advantages such as rapid response time. Polyacrylamide has extremely long response times. Poly (chloromethyl) styrene was rejected as an option as its hydrophobic surface tended to produce results that were not reproducible [9]. In general, polymers as a substrate for immobilising optically active indicators exhibit significant degradation in the presence of strong acids or bases. Moreover, they are also less tolerant of the high temperatures or pressures typically encountered in many industrial and practical applications [10]. A new

technique for avoiding some of these difficulties relies on solution-deposited films, which can be conveniently doped with organic compounds such as laser dyes that would be decomposed in other methods of film depositions [11]. The sol-gel technique (the hydrolysis of an organometallic precursor followed by condensative polymerisation) results in chemical indicators bound in a highly durable matrix. Long-lasting and environmentally ruggedised fibre optic sensors result from this process which are stable, reversible and highly sensitive. Two problems remain: surface effects and response time. The reagent often reacts to the surface levels of the analyte rather than that of the analyte in solution. Response time of a sol-gel matrix is largely determined by the mass transport characteristics and is thereby slow. Nonetheless, sol-gel has the potential to be used to produce tailor-made glasses and ceramics with wide-ranging applications [12].

Sol-gel has been used by other researchers in an intrinsic (but non-tapered) evanescent fibre optic pH sensor. Results, as seen in Figures 1 and 2, are encouraging.

A tapered fibre, with greater exposure of the evanescent field, is likely to produce even better results.

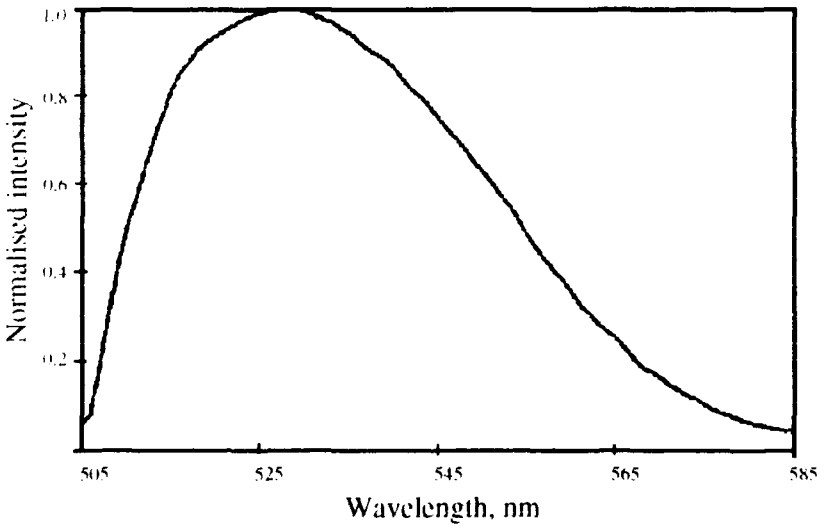

Figure 1: Evanescent Wave-Excited Fluorescence of Fluorescein in Sol-Gel [13]

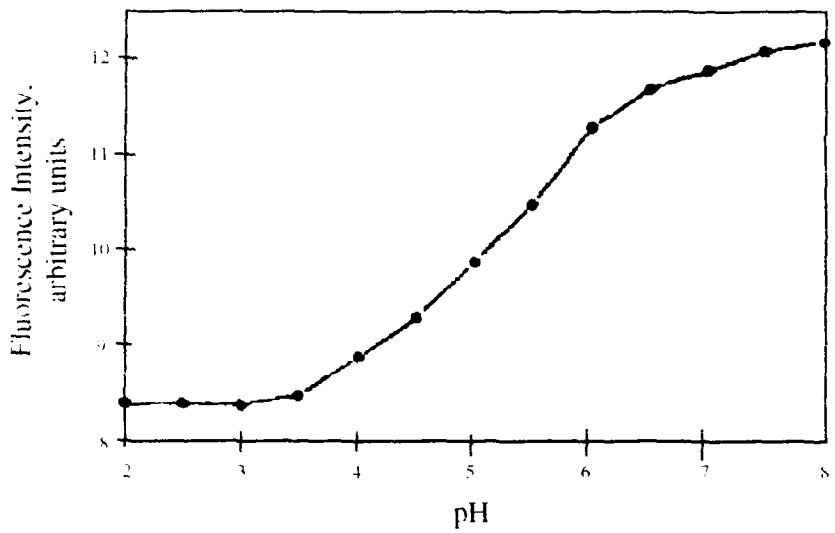

Figure 2: pH Sensitivity of Sol-Gel Sensor[14]

2.3 pH Sensors:

As the previous figures indicate, pH detection is a viable application for optical fibres. The measure ient of pH is very important in chemical systems and where limitations of conventional pH electrodes make them unsuitable for certain applications, fibre optics can be used.[15] Optical sensors also offer good mechanical flexibility, very small size, and more precise measurement of extreme values of pH.[16] Further, in acidity detection in the blood and in the stomach content, optical sensors can be used for "in vivo" measurements.[17]

Since the surface of the waveguide tends to be polar, hampering measurements in ionic solutions, a coating of some sort on the surface of the optical fibre would serve to not only minimise this effect but also immobilise the fluorescent indicator. pH sensors with optical fibres will not necessarily measure pH itself, but rather pKa, depending on the chemical process chosen to interact with the external media. Calibration measurements would have to be established in order to describe the relationship between the chemical reaction taking place in the coating on the surface of the fibre and the actual level of pH. Immobilised fluorescent indicators that have a known rate of conversion from one form of the indicator to another accompanied by a color change that is monitorable by a fibre are a

very reasonable choice. The method most often used for attaching such an indicator requires a silanisation process. This method avoids almost all reagent loss and a shift in the pK value and a broadening of the detectable pH range can often be observed.[18]

2.3.1 Theory and operation:

A major disadvantage of photometric pH measurements is that it is the concentration of a dye species which is determined and related to pH, not the concentration

$$[I^-] = \frac{cK}{(10^{-pH} + K)} \qquad \textit{Equation 1}$$

I- = the conjugate base of the indicator

c = the concentration (strictly speaking should be activity; holds true for dilute solutions; $<10^{-5}$M)

K = the equilibrium constant

Figure 3: Relationship of Indicator Activity to pH

of hydrogen ions itself. The colour of the dye, which is usually a weak acid such as a phenol, is governed by its pKa as well as the actual pH value. This pKa can be affected by external factors such as ionic strength. [19] An indicator, usually represented by the form HI, acts in solution as described by Figure 3.

At low pH values, the equation approximates to [I-] = 0. At high pH values, [I-] is equal to c, the concentration. Consequently, a plot of [I-] and the absorbance strength against pH follows a sigmoid shape, similar to that of an acid-base titration. [20]

2.4 Optical fibres as Waveguides:

Before going further, we need to discuss the characteristics of the optical fibre as a waveguide. The fibre consists of the three parts: the core, cladding, and protective outer coating. In our application, the outer coating is removed. The cladding becomes thinner and elongated during the tapering process.

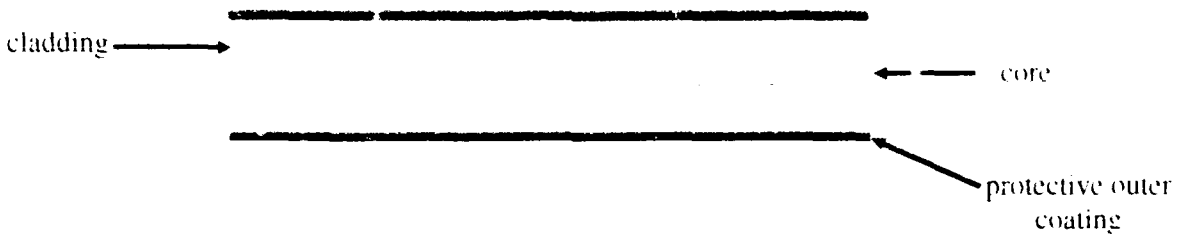

Figure 4: Optical Fibre Configuration

The York single-mode fibre used guides light predominantly in the core. The optical radiation also has an associated evanescent field that is a rapidly decaying exponential. The extent of this field is directly proportional to the wavelength of the radiation in the core and inversely proportional to the number of TE modes supported by the core. The evanescent field can react with the material of the cladding in the same manner as if it was a real field. In a tapered fibre, the external media acts as the cladding at and near the taper waist, thus providing the basis for interaction. To maintain maximum field strength, single mode fibres would be preferred for the construction of evanescent field sensors. [21]

2.4.1 Exploiting the Evanescent Wave:

Specific techniques for making use of the evanescent field of a waveguide in sensing applications are well-developed. One form of chemical analysis using evanescent wave interactions at the surface of a crystal waveguide relies on the penetration of the evanescent wave of a totally internally reflected ray into an absorbing sample medium. The amount of absorption depends on both the amplitude of the evanescent field in the sample medium and the number of reflections within the waveguide sample cell. The former increases dramatically for incident angles approaching the waveguide sample critical angle, and the latter is inversely proportional to the waveguide thickness. An unclad optical fibre is a particularly useful sensing element in that its relatively narrow core diameter provides a large number of reflections per unit length. [22] Once the evanescent field has interacted with the external solution via immobilised indicators a certain level of fluorescent light is

generated. As the external solution is acting as the cladding, this fluorescent light originating in the solution can indeed be coupled to guided modes in the fibre core and transmitted over long distances without appreciable loss.

The coupling of fluorescent energy generated in the fibre cladding to guided modes in the core can be appreciable, especially for fibres with large V numbers. The dependence of coupled fluorescence intensity on fibre length is nonlinear: there is an upper limit on the amount of fluorescent power which can be coupled to guided modes in the core. [23] The efficiency of the coupling of cladding fluorescence to the guided modes depends strongly on the "V number" of the fibre:

$$V = \frac{2\Pi}{\lambda} * a(n_1^2 - n_0^2)^{\frac{1}{2}}$$

$$NA = (n_1^2 - n_0^2)^{\frac{1}{2}}$$

λ = vacuum wavelength of the guided light

a = radius of the fibre core

NA = Numerical aperture

n_1, n_0 = indices of refraction of the core and cladding, respectively

Figure 5: Normalised Frequency of Optical Fibres

Fibres with higher V numbers exhibit strongly coupling coefficients since these fibres have a larger number of modes near cutoff and the evanescent fields of such modes penetrate more deeply into the cladding. [24] However, higher V numbers reduce the absorbance of the evanescent wave. Experimental work has been performed to determine the wave behaviour and power capture back into the core guided modes of the adiabatically tapered fibre.

2.4.2 Wave behaviour in tapers:

In a tapered fibre, as the lowest order fibre mode propagates through the taper its spot size increases until the modal field is guided primarily by the fibre cladding and the external medium surrounding the taper waist. After passing through the taper waist the cladding mode evolves once more into a core-guided mode. A strong optical interaction can occur with the medium surrounding the taper. [25]

The interaction is particularly strong in the tapered fibres used in this lab as the waist diameter is extremely small. The optical power density in the evanescent field of a micron taper is about three orders of magnitude higher than can be achieved by polishing away the cladding of a standard single-mode fibre. [26] Biconical fused fibre adiabatic tapers can be made with a waist diameter of less than 1 m, and a transmission loss than 0.1 dB. [27]

With a taper of waist diameter of about one micron surrounded by a solution of refractive index 1.44, an input power of only 10W will produce a power density in the evanescent field at the taper waist of about 200kW/cm2 at a wavelength of 650 nm. [28] This extremely intense level of optical energy is ideal for sensor interactions, as it provides for high signal-to-noise ratios and thereby readily extractable information.

2.5 Reagents for Interaction:

Fluorescent substances or absorption indicators can be used for the detection of pH by optical fibres. Many dyes have colours that are sensitive to hydrogen-ion concentration and thereby give optical information about the pH of a solution. If an indicator of the form [HI] dissociates into [I$^-$] of a different colour than that of [HI], the overall colour of the solution will be a result of the predominance of one species or another. Fluorescence detection for sensing offers greater sensitivity but less resistance to interferents and thereby a decrease in the accuracy of the measurement. Although less sensitive, absorption indicators show negligible interference response. [29] The end application and sensor configuration

determine whether a fluorescent or absorption indicator would best suit the configuration. In the pH sensor described here, I used a fluorescent indicator.

2.5.1 Fluorescent indicators:

A fluorescent indicator typically absorbs incident light of one wavelength and re-emits at a higher wavelength. The differential between the two can be as little as 25 to as much as 180 nm. Although it is desirable to have very distinct peaks in order to isolate the source from the emission, the efficiency of the indicator, and thereby the optical intensity, can allow for distinguishing between even very close wavelength peaks. Although typical pH ranges for optical reagents are 1-2 pH units in solution and 2-3 pH units in immobilised structures[30], some indicator dyes exist in several chemically and optically separable forms at various levels of pH, broadening the detectable pH range. Mixing together more than one reagent could also achieve the same result.

2.5.1.1 Fluorescein:

Fluorescein, or Uranin as a laser dye, is an exceptional fluorescent indicator. It is a dye of the xanthene type. The molecular structure and spectral properties of these dyes are very susceptible to the pH value of solutions and the polarity of solvents. The typical

FL: Fluorescein (disodium fluorescein)

FLCl4: Tetrachlorofluorescein

EO: Eosin

CY: Cyanosin

ER: Erythrosin

RB: Rose bengal

MR: Merbromin

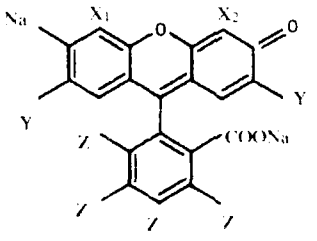

FL: $X_1 = X_2 = Y = Z = H$

FLCl4: $X_1 = X_2 = Y = H$; $Z = Cl$

EO: $X_1 = X_2 = Y = Br$; $Z = H$

CY: $X_1 = X_2 = Y = Br$; $Z = Cl$

ER: $X_1 = X_2 = Y = I$; $Z = H$

RB: $X_1 = X_2 = Y = I$; $Z = Cl$

MR: $X_1 = H^2$; $X_2 = HgOH$; $Y = Br$

Figure 6: Fluorescein and its Variants[31]

four-ring structure, as seen in Figure 6, has a dissociable carboxyl group at the 2' and an aryl hydroxyl at the 6 position.

All of the above configurations may be used as indicators.

Flourescein (disodium fluorescein) may exist in one of six forms depending on pH value. Four of these forms are quite optically distinct, as seen in Figure 7.

pH	λ max(nm)	Form
1-2	438	protonated cation (p.c.)
4.003	450,475	p.c. + neutral quinoid
6.86	495	anion I, II
9.28	495	anion II

Figure 7: The Chemical Forms of Fluorescein at Various pH Levels [32]

In strong acidic solutions the wavelength of maximum absorbance is 438 nm, but the resultant fluorescence is not very intense. In a neutral to slightly basic solution, absorption peak is near 495 nm. In strongly basic solutions, the maximum absorption peak is again 495 nm but the fluorescence level is extremely intense. In terms of deprotonation, this can be expressed as in Figure 8:

$$\text{Fluorescein: } \underset{\text{no absorption}}{\text{Lactonic(VI)}} \longleftrightarrow \text{quiniod} \overset{-H+}{\longleftrightarrow} \text{anion I (VII)} \overset{-H+}{\longleftrightarrow} \text{anion II (VIII)}$$

Figure 8: The deprotonation of Fluorescein [33]

Similar results, as seen in Figure 9, have been seen by other researchers, even when fluorescein is in a non-aqueous medium.

The level and position of fluorescence available can change based on concentration. In many dye systems complications due to dimer formation may arise. The fluorescein dimer has two absorption peaks, at 468 and 508 nm, and a minimum between these two peaks

Medium	pH or T	Concentration [M/L]	λ max absorption (nm)
Water	1	10^{-4}	437
Water	6	10^{-4}	479
Water	13	10^{-4}	490
Thin Film	unheated	10^{-3}	455
Thin Film	200°C	10^{-3}	490

Figure 9: Fluorescein Absorption in Water and Thin Films [34]

around 488 nm. The dimer should exhibit a lower fluorescence than the dianion monomer when excited with 488 nm light. Therefore, the pH responses of fluorescein above pH 7, where most fluorescein molecules are dianions, will strongly depend upon the dimerisation of the dianion. [35] In disodium fluorescein, dimer formation is not observed at concentrations lower than 10^{-3} mole/L. [36] The variation in fluorescent wavelength is as described by Figure 10.

Dye concentration (M)	λ emission, nm
10^{-3}	535
10^{-4}	520
10^{-5}	506
10^{-6}	503
10^{-7}	504
10^{-8}	500

Figure 10: Emission wavelength shift with concentration. Excitation wavelength is 450 nm. [37]

In summary, as the pH increases, the wavelength for maximum absorbance by fluorescein shifts from 435 to 495 nm; and the fluorescence maxima decreases from approximately 555 to 530 nm for a solution of 10^{-3} M. To bias the sensitivity curve of the sensor so that high fluorescence values are seen at high pH levels, the upper ends of both limits should be used.

3.0 Experimental Design:

3.1 Experimental Optimisation:

In order to establish if tapered single-mode fibres would be responsive to pH changes while immersed in a dye cell with a pH-sensitive dye, the various subcomponents of such an experimental system had to be first determined and subsequently optimised. These components included the laser wavelength, the dye concentration, the fluorescence maxima, the taper thickness, as well as the automation of data collection. The dye to be used, disodium fluorescein or Uranin, was a key figure in determining the appropriate excitation laser wavelength. Uranin exhibits different absorption maxima in different solvents, as well as at different pH levels. In order to obtain absorption spectras, the following system was used:

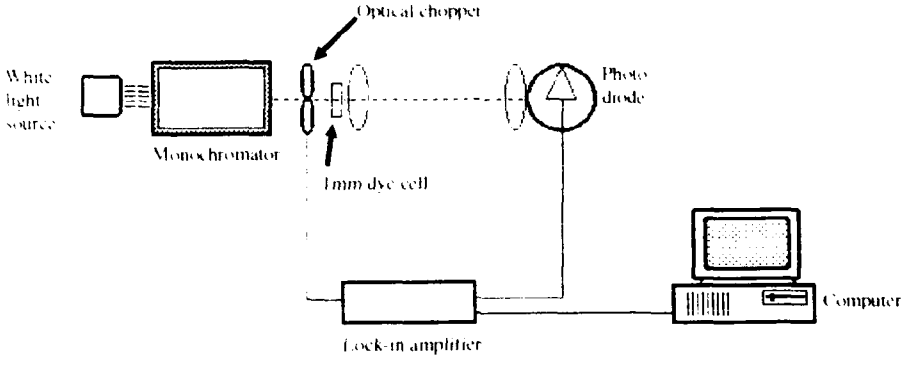

Figure 11: Absorption Spectra Measurement System

3.1.1 Excitation Wavelength:

The wavelength of the white light source was varied by adjusting the monochromator. The ensuing beam illuminated the dye cell and the remaining (non-absorbed) light was captured by a large area photo diode. This light level was monitored by a lock-in amplifier and recorded on a computer. The emitted level of light was

measured at every wavelength by filling a dye cell with the solvent. Absorption of the dye was measured by placing dye and solvent in the dye cell and looking at the difference between the first and second measurements. This procedure was repeated at three pH levels (4, 7 and 10) using buffer solutions in addition to the dye. While taking these measurements, the room was darkened and the optical elements from the monochromator to the photo diode were shielded by aluminum tubing to minimise interference with ambient light.

3.1.2 Dye Concentration:

Dyes at very high concentrations, as noted earlier, can form dimers, which depress the total level of fluorescence. In such a case, a typical absorption spectra is not seen, as shown in the figure below.

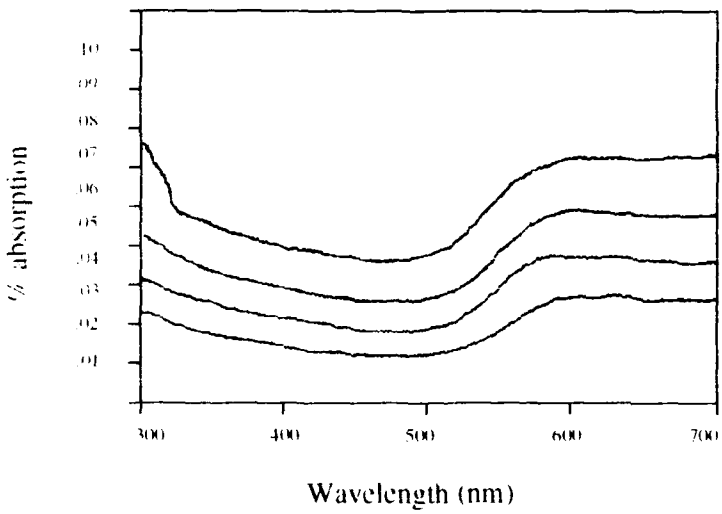

Figure 12: Dimer Absorption Spectra

The total dimer fluorescence measured was two orders of magnitude lower than that taken at more dilute concentrations. Concentrations above $2x10^{-2}$M tended to form dimers. Once a lower concentration ($1.02x10^{-2}$ M) was used, more typical absorption spectra were obtained as seen in Figure 13.

The two well-defined absorption peaks correspond to different forms of Uranin. The maxima at approximately 440 nm corresponds to the dye's cation and ampho ion. The maxima at 490 nm indicates the presence of the anion II form of the dye. Between the two maxima is a high level of absorption with no clearly discernible maxima: this corresponds to

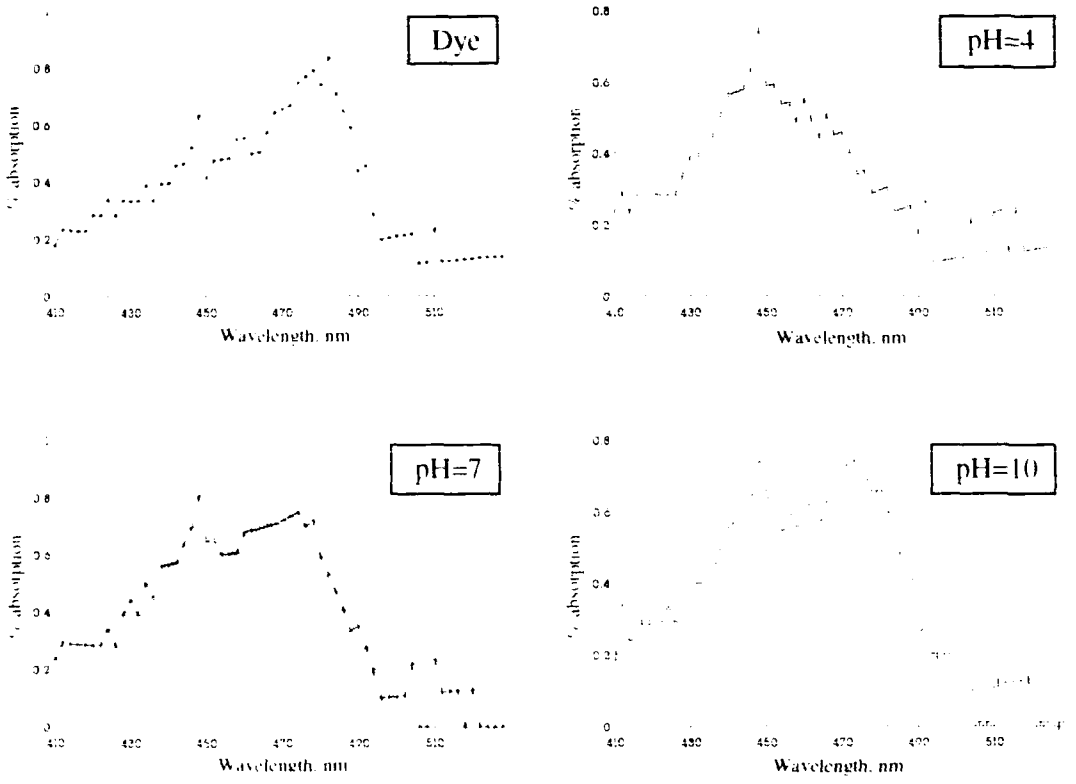

Figure 13: Fluorescein Absorption Spectra: Dye, pH = 4, 7, and 10

the quinoid and anion I forms of the dye that are seen at near-neutral pHs, often with an absorption maxima of about 470 nm.

3.1.3 Fluorescence Maxima

Various environmental factors will alter the fluorescence maxima of Uranin. The concentration of dye determines the total level of fluorescence observed as well as where the fluorescence is seen. The pH level of the solution has a drastic effect on the level of

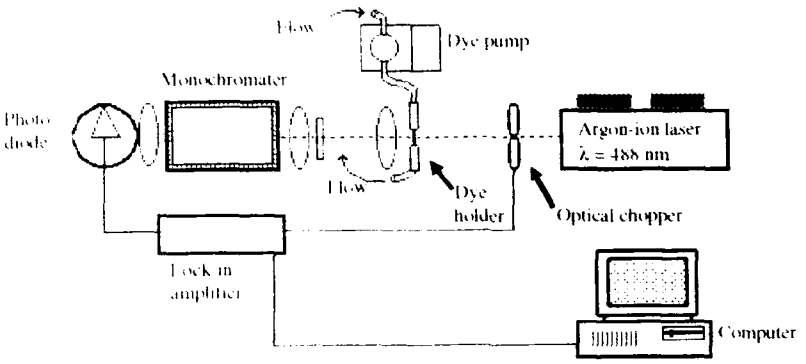

Figure 14: Bulk Fluorescence Measurement Setup

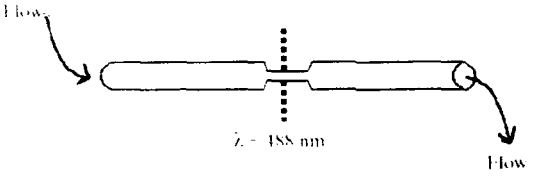

Figure 15: Overhead view of Dye Circulator

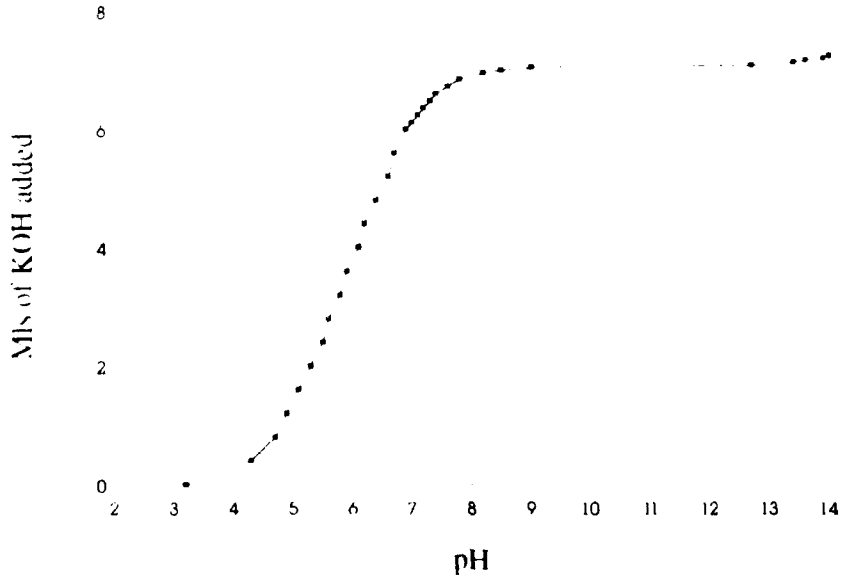

Figure 16: Titration Curve: 100M KOH vs 17.4 M Acetic Acid

fluorescence measured. The fluorescence spectra at the concentration chosen as a result of the absorption measurements was taken,without a taper, to determine the maxima. A method for circulating the dye through the laser beam was developed, as shown in Figure 14.

The fluorescent light resultant from the dye was collimated as best possible and sent through a monochromator. A wavelength scan was performed to determine the peak fluorescence wavelength. In order to filter out the source wavelength, an OG515 optical filter was used. The fluorescence spectra was determined at various pH levels. A titration curve as a baseline was obtained by adding 100M KOH to 17.4M acetic acid. This curve, as seen in Figure 16, displayed a typical sigmoid shape.

Fluorescence maximas at pH 2-14 were recorded to establish a wavelength of

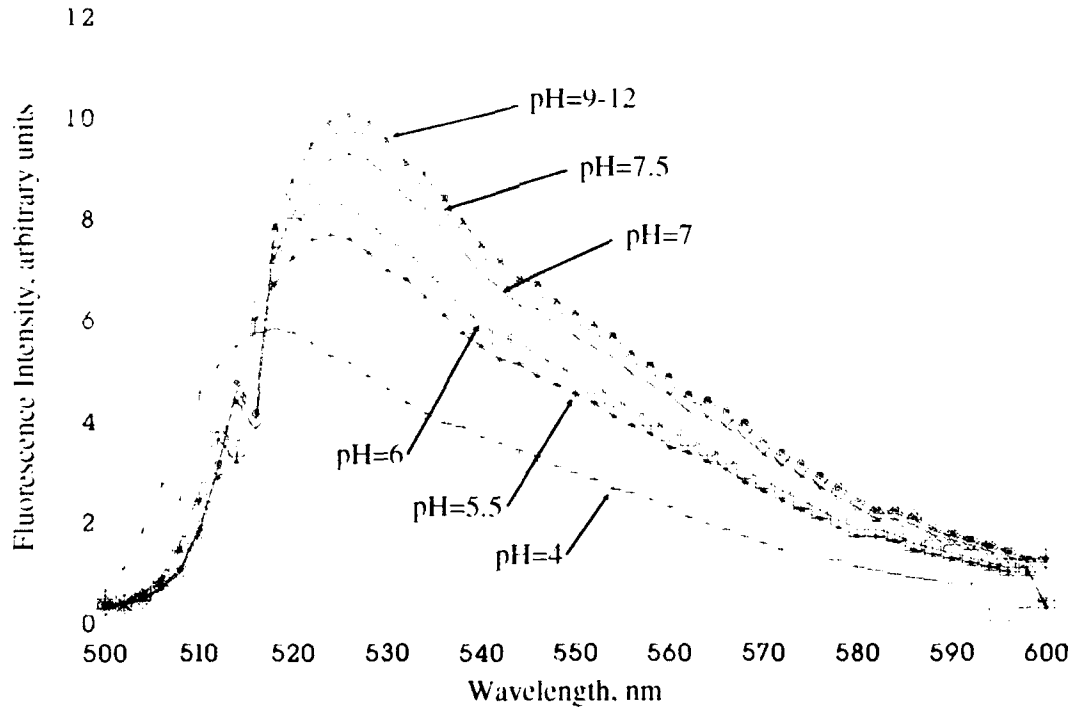

Figure 17: Fluorescence Sprectra of Uranin

maximum emission. As Figure 17 shows, the overall shape of the curve remained the same.

but the fluorescence level decreased with lower pH. Further, the fluorescence maxima shifted slightly to the left as the pH decreased.

The maximum fluorescence level was measured at 526 nm. Once this maxima had been established, a titration was performed, using a pH meter to verify the pH levels, and plotted against the fluorescent intensity measured. This would demonstrate if the activities actually measured by fluorescent capture were comparable to the hydrogen ion levels seen in the baseline acid-base titration. As seen in Figure 18, the fluorescent levels were very low in acidic regions, increasing to a peak at approximately pH=9.

3.1.4 Taper Diameter:

Taper measurements were expected to be higher as the fluorescent light would be captured directly into a fibre. A highly sensitive yet durable taper had to be fabricated.

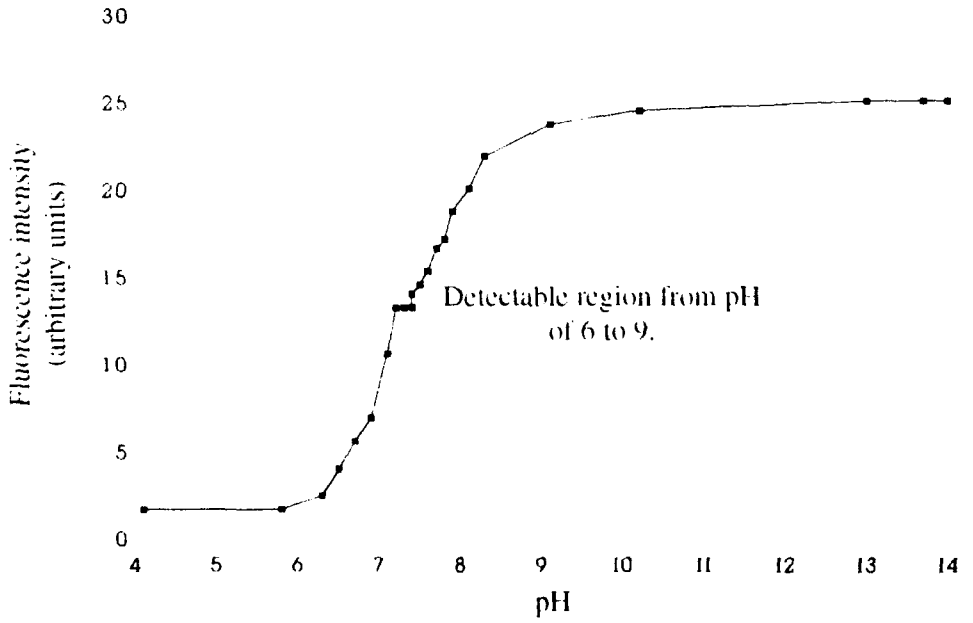

Figure 18: Bulk Fluorescence of Uranin vs pH

The tapers were prepared in the established method, using single-mode SM450 York fibre, with a numerical aperture of .18, a cutoff wavelength of 450 nm, and a fibre outer diameter of 80 microns. The tapering system used was as illustrated in Figure 19.

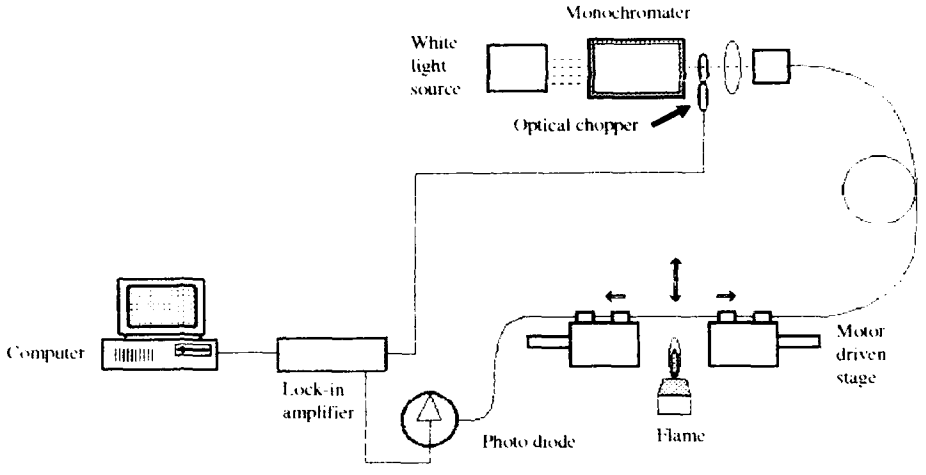

Figure 19: Tapering Rig

careful use of a razor. This unprotected section is then cleaned with acetone and placed above an oxybutane flame. The fibre is held in place with carefully aligned blocks and magnetic strips. The flame is then slipped into place directly below the fibre and the motors engaged to stretch the fibre. Transmission loss is monitored via computer. The fibre was stretched until the waist diameters were anywhere from .5 to 10 microns in diameter. An

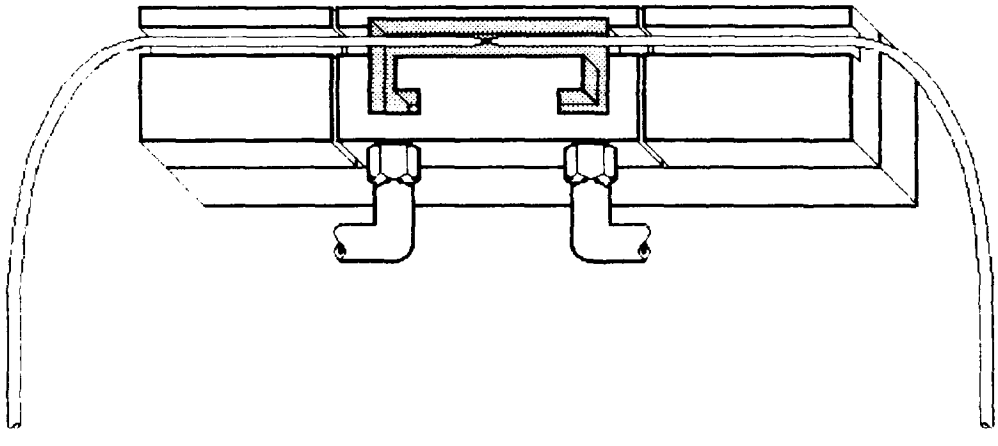

Figure 20: Taper Mount with Dye Cell

approximate size was determined during tapering with a stereoscopic optical microscope. Once mounted, the taper diameter was verified with a more accurate microscope. The mount for the taper was as used in previous work and is illustrated in Figure 20.

Only tapers with less than .1 dB loss were used. A typical loss spectrum is seen in Figure 21. The appropriately low-loss tapers, once mounted, could be connected to a dye reservoir and a pump in order to circulate Uranin dye and various solutions.

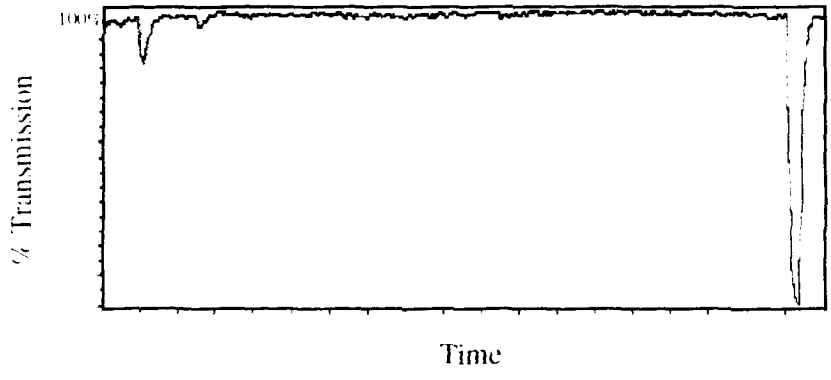

Figure 21: York Fibre Loss

3.1.5 Components of the Dye Solution

The elements of this circulating solution were chosen carefully to maintain a constant index of refraction. Other constraints on the solution included the physical size of the dye reservoir and the necessity for a constant aliquot of Uranin. The indices of refraction of the dye and titrate (or buffer) were added volumetrically and enhanced optically through the use of a high refractive index solution. These solutions tended to be viscous and exhibited unpleasant properties: benzyl alcohol always broke tapers after a very short time of circulation, and all solutions tended to mix slowly and not entirely uniformly. Dimethyl sulfoxide (DMSO) was most successful: tapers 4-5 microns in waist diameter survived its circulation. Uranin had the index of refraction of its solvent, methanol, or 1.326. The index of refraction of DMSO was relatively high, with n=1.478. Glacial acetic acid (17.4M) was

typically low in refractive index at 1.37; all of the buffers were similarly low at 1.32. The index of refraction for 100M potassium hydroxide (KOH) was not initially known. The index of refraction of organic substances, in general, is affected by its concentration, as demonstrated in Figure 22.

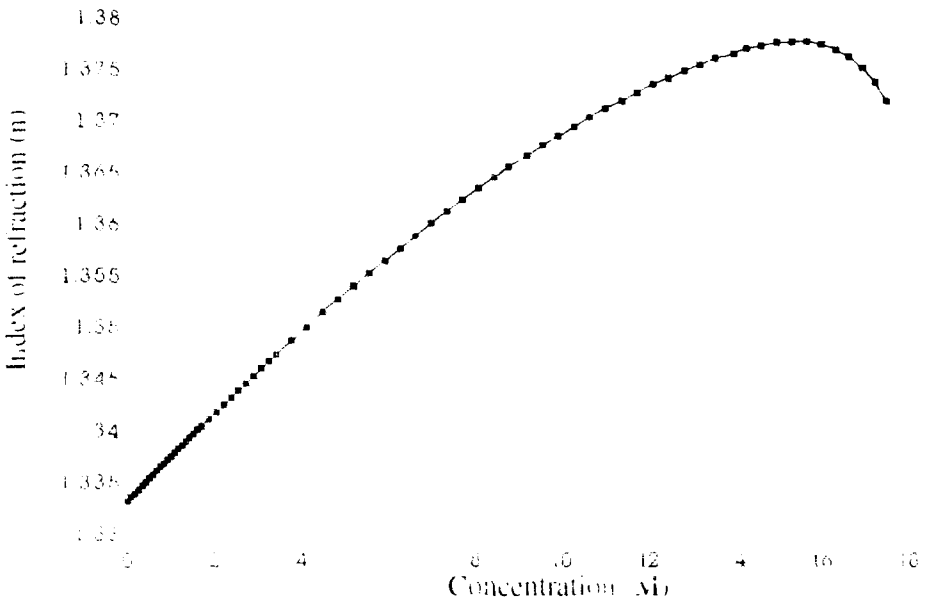

Figure 22: Index of Refraction vs Concentration, Organic Substances[38]

It was not known at which concentration of KOH the peak level of refractive index would be seen, nor what the peak was, though the known data are as described in Figure 23.

In order to determine the index of refraction for 100M KOH, a refractometer and low and high index solutions were used. The simple refractometer used only had a range from n=1.43 to 1.48. Volumetric titrations with methanol (low index) and DMSO (high index) were separately carried out, as the index of refraction of 100M KOH could have been on either side of the end points of the refractometer. The determined refractive index was 1.4. Once this had been established, an appropriate table of solutions required for each pH level to maintain the same refractive index could be derived as seen in Figure 24.

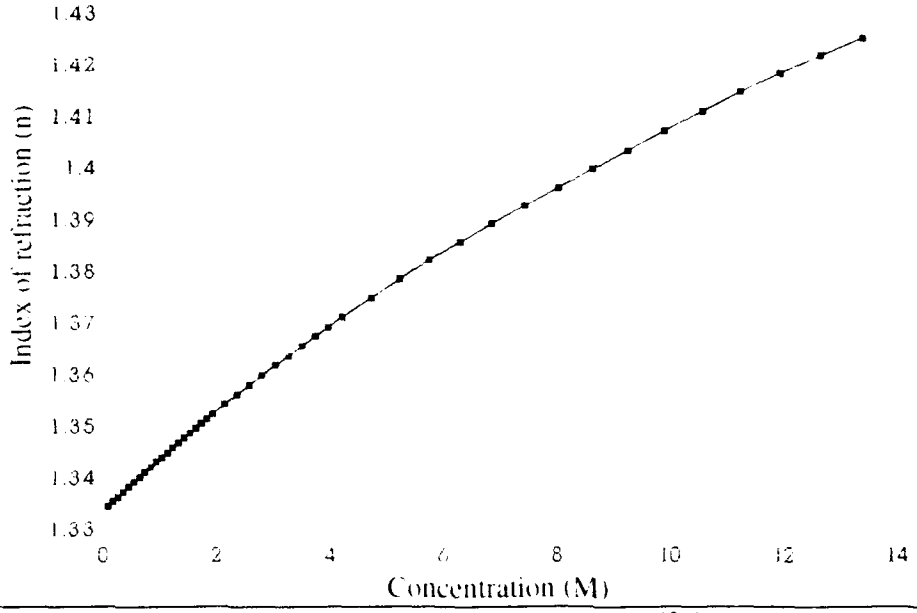

Figure 23: Index of Refraction vs Concentration, KOH[39]

3.2 Data Collection System

In order to automate collection of analog data from the experimental system, a data acquisition card was installed in an IBM-compatible AT computer. Connections were made to provide for analog input as well as digital output. The analog input was connect to the lock-in amplifier to directly record the received voltage levels. Conditioning software was written to scale the data appropriately. Digital output was provided to drive a stepper motor connected to a monochromator. Several comparative "test runs" were performed to verify data read in to the computer matched data measured by the lock-in amplifier. Once

pH	DMSO (mls)	Uranin (mls)	Buffer (mls)	Acetic Acid (mls)
2.1	32.1	10	0	3
4	30.5	10	2.5	0
7	30.5	10	2.5	0
10	30.5	10	2.5	0

Figure 24: Sample solution mixtures for n=1.44:
proportions for other pH values were similarly determined .

experimentally verified, all data was taken was recorded on the computer. Appendix II contains detailed descriptions of elements within the data collection systems.

4.0 Results:

4.1 Final Experimental System:

The response of the taper to pH as measured by evanescently-excited fluorescence levels was determined using the system seen in Figure 25.

Based on earlier results, each portion of this system had been optimised to the extent possible. The tunable argon-ion laser was set to 488 nm, the wavelength most appropriate for absorption maxima of the dye. All optical elements were aligned so that the maximum amount of light was retained from the laser beam. The fibre ends were cleaved and placed in the x,y,z micropositioners to receive or emit the maximum signal. The dye solution was at a fixed (and high) index of refraction of 1.44 that would allow the evanescent wave at the taper waist to interact with the surrounding media and also foster recapture at the

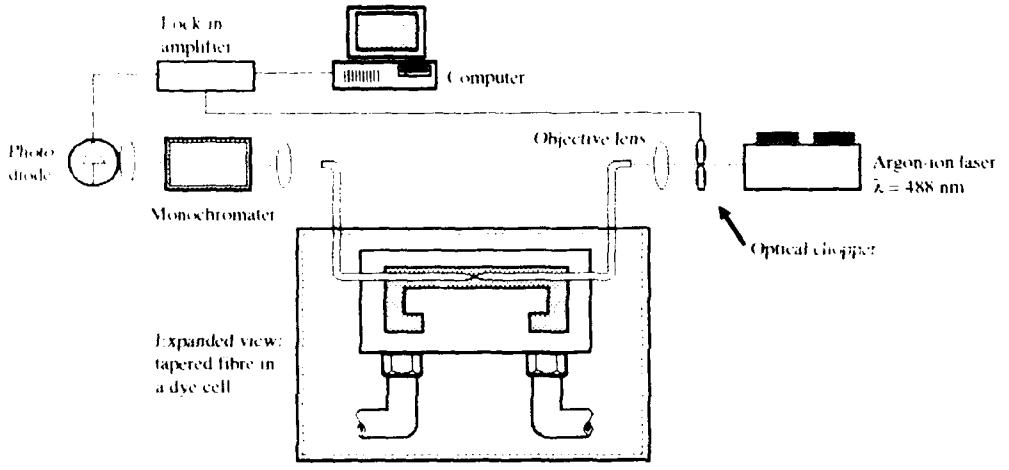

Figure 25: Taper Setup of pH Measurements

far end of the taper. The concentration of Uranin at $1.02x10^{-2}$M was high enough to get a significant fluorescence signal without formation of dye dimers. The dye was circulated around the taper at a slow enough speed, controlled by extending the length of the tubing from and to the dye reservoir, to minimise breakage of tapers. The 4-5 micron waist diameter taper was small enough to allow interaction of its evanescent field with its external medium and large enough to be physically and chemically durable with the viscous solutions used to maintain the refractive index.

Wavelength	Dial Setting	Wavelength	Dial Setting
771	18.7	501	48.8
751.5	21	496	49.1
744	21.8	488	50
732	23.3	476	51.2
714	25.2	472	51.6
708	25.8	465	52.3
697.5	27	457	53
685.5	28.3	454	54.5
681	28.9	316.4	67
632.8	34.5	258	72.1
514	47.5	250.5	72.6

Figure 26: Monochromator Dial Setting and Wavelength Correspondence

The monochromator had been aligned with all wavelengths of the tunable argon-ion laser and a polynomial fit established. The monochromator could then be verifiably set at 526 nm to ensure maximum fluorescence signal.

4.2 Taper Response to pH:

Once final optimisation was complete, several sets of data were taken on the same set up with the same taper. These all showed the sigmoid form as expected and indicated in Figure 27.

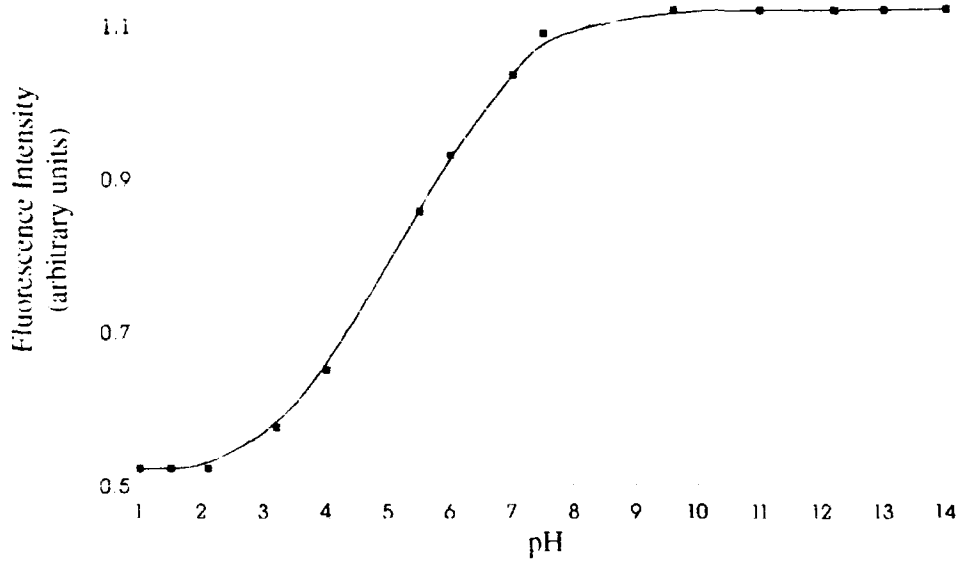

Figure 27: Taper Response to pH

Signal levels of fluorescence were much higher than those recorded in bulk fluorescence measurements. The higher signal levels extended the detectable range to pH 3.2-9, as Figure 28 demonstrates.

4.3 Discussion:

The viability of using an adiabatically tapered optical fibre as a pH sensor has been shown. Although the system in use required a constant index of refraction to keep all fluorescence levels comparable, the final response curve clearly follows that of hydrogen ion sensitivity. The extended range of the sensor and its increased signal levels over those results seen in the bulk fluorescent system reflected the increased efficiency with which the light was collected.

The configuration of this device as an intrinsic sensor makes it very attractive for further optimisation. The system already meets some of our requirements of a good sensor in that it is sensitive, inert to the external media, reversible and chemically robust. It does,

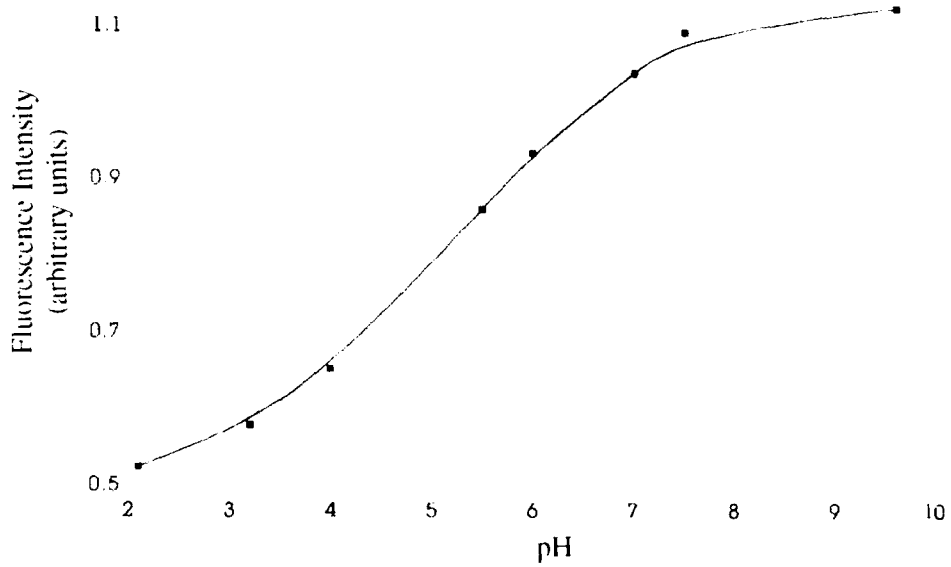

Figure 28: Detection Regime for Taper

however, require pretreatment of the sample (and thereby calibration) and is not necessarily selective. Suitable support structures, such as sol-gel, could be used to create a device that does not require a fixed external index of refraction and aliquot of Uranin dye. An immobilisation coating would have to be chosen with care in order to retain the responsitivity of the sensor.

5.0 Future efforts:

Several areas of work are natural extensions of this preliminary research. The tapered fibre should be made sensitive to chemical species other than the hydrogen ion, in order to isolate sensor response from other factors, such as ionic strength effects. Another area of interest for the taper is the exploration of the behaviour of colloidal solutions. Lastly, other sensor configurations should be examined, both experimentally and theoretically.

The current system configuration of the tapered fibre could be readily adapted for the detection of other substances. A different indicator dye could be used that also exhibits a high level of absorbance for the wavelengths of the argon-ion laser. One such dye is fura-2, which is sensitive to the concentration of calcium.

Another taper interaction for investigation is the non-linear optical property of metal colloids. Gold and silver colloids exhibit a dramatic resonantly enhanced third order nonlinearity, $\chi(3)$. This effect is related to the surface-mediated enhancement at the plasma frequency. [40] The index of refraction of such colloids would have to be stabilised as before. Surrounding a suitable taper with metal colloids would also allow the demonstration of compact fibre-based phase conjugate oscillators and amplifiers.

Different sensor configurations should be attempted as well. Characterisation studies of sol-gel coated tapers, supplied by Dr. Henry, could be performed. Further, once design criteria for the second type of sensor, capable of detecting calcium (for example), have been determined, these too could be coated and subsequently characterised. These two data sets could form the basis of a rudimentary baseline for comparison of the effectivity of sol-gel coated tapered fibres.

Configurations separate from the single tapered fibre are worth investigating as well. Using suitably designed optical couplers, excitation wavelengths of the laser could enter one arm of the coupler, interact with a solution as established in the initial work, and re-emerge at fluorescent wavelengths from the opposite arm. This would be examined theoretically and experimentally.

Finally, it would be possible to use a "drilled core" sensor configuration. [41] In this instance, a large glass rod could be drilled to allow various cylinders of different materials to placed within the overall waveguide. Again, the far end of this waveguide could

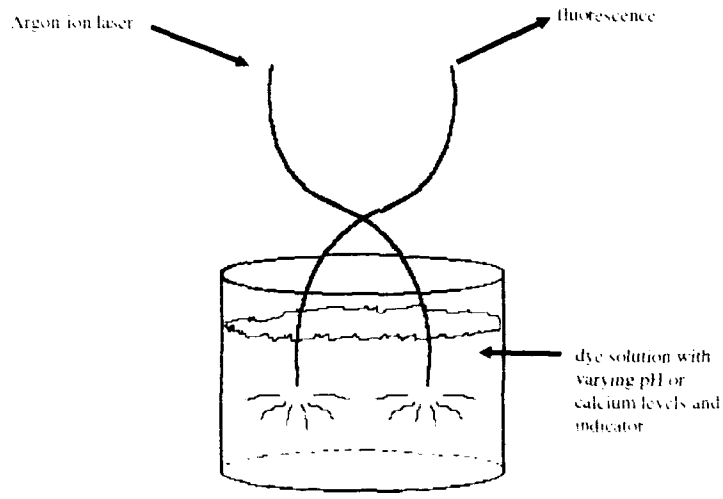

Figure 29: Potential Coupler Configuration

be placed in a solution, and fluorescent light guided up the second path. This too would be examined theoretically and experimentally.

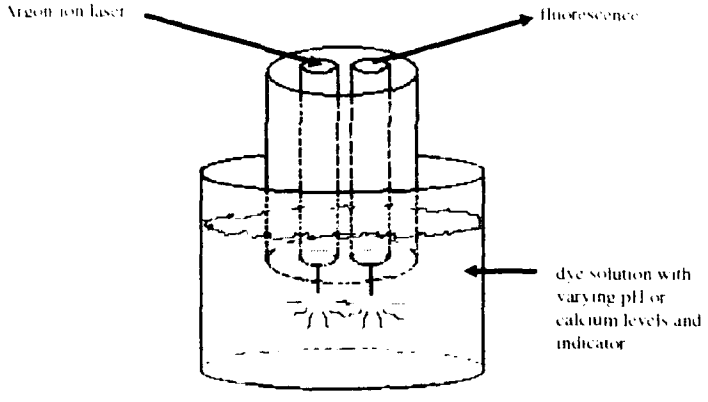

Figure 30: Potential drilled-core sensor

In order to most effectively time-phase these efforts, taper work would be performed first. This would logically be followed by efforts to examine coupler sensors. A final effort would be devoted to the drilled-core configuration. All efforts will likely take between six and eight months each, leaving time for suitable write-ups and analysis.

Appendix I
Glossary

Aliquot: An exact amount of solution.

Amphoteric (or ampho): Able to function both as an acid and as a base.

Analyte: Substance under analysis.

Anion: Negatively charged chemical species (ions).

Aqueous: Dissolved in water.

Aromatic ring: Carbon ring in which the carbon atoms are arranged in loops, with double and single bonds alternating. Frequently depicted as a regular hexagon. Aromatic refers to the fact that several compounds of this type are fragrant (for example, naphthalene).

Aryl hydrogen: Hydrogen directly bonded to an aromatic ring.

Buffer solutions: solutions that contain both acid and base and can respond to the addition of either, in an attempt to maintain a constant pH.

Carboxyl group: the chemical group COOH.

Cation: *Positively charged chemical species (ions).*

Deprotonation: subtraction of the hydrogen ion (sometimes called dehydrogenation)

Dimer: a compound composed of two specified atoms or molecules.

Glacial acetic acid: Pure acetic acid

Hydrolysis: a hydroxyl ion becomes attached to the metal (for instance) ion.

Hydroxyl: the univalent radical or group, OH.

Indicator: any of various substances that indicate a presence, absence or concentration of a substance by means of a characteristic change (usually colour).

In vivo: processes carried out in the living organism.

Ionic: a substrance that is electrically charged by the local loss of one or more electrons (see polar)

Organic compound: chemical compound formed from carbon.

Phenol: any of a class of organic compounds whose molecules contain one or more hydroxyl groups bound directly to a carbon atom in an aromatic ring.

pK: K represents the dissociaton rate of a given substance, i.e., acetic acid molecules and acetate ions:

$$\frac{|H^+||C_2H_3O_2^-|}{|HC_2H_3O_2^-|} = K$$

$$pH = pK - \log \frac{|HC_2H_3O_2|}{|C_2H_3O_2^-|}$$

It is this last term that can cause the pH reading to be inaccurate if the concentration of an ion other than hydroxyl is measured.

Polar: (a molecule) having an uneven distribution of electrons and thus a permanent dipole moment.

Reagent: any substance used in a chemical reaction to detect or measure other substances.

Silanisation: formation of any of various silicon hydrides (Si_nH_{2n+2}).

Sol-gel: a chemical process in which a single or multi-component metal oxide solution undergoes gelation (colloid of a more solid form) to form a coherent rigid network of the oxides present.

Solvent: a liquid capable of dissolving another substance.

Titration: the process of determining the concentration of a substance in solution by adding to it a standard reagent of known concentration in carefully measured amounts until a reaction of definite and known proportion is completed and then calculating the unknown concentration.

Xanthene dye: any various brilliant fluorescent yellow to pink to bluish red dyes characterised by the heterocyclic compound $C_{13}H_{10}O$.

APPENDIX II
Equipment Listing

The equipment used in this investigation is listed by major subject group: optical, electronic, and chemical.

OPTICAL

Laser

Omnichrome air-cooled Argon-ion laser, model-543. Continuous wavelength; can operate in single line or multi-mode.

LINES AVAILABLE

Wavelength (nm)	Power available (mW)
454	5
457	27
465	28
472	18
476	35
488	120
[illegible]	25
501	12
514	100

Figure 31: Multiple lines of the argon-ion laser

In practice, the power levels used are approximately half of the above.

Fibre

York single-mode fibre, SM-450. Cutoff wavelength is 450nm. Fibre outer diameter is 80 microns. Numerical aperture is .18

Refractometer

Bellingham & Stanley sugar refractometer.

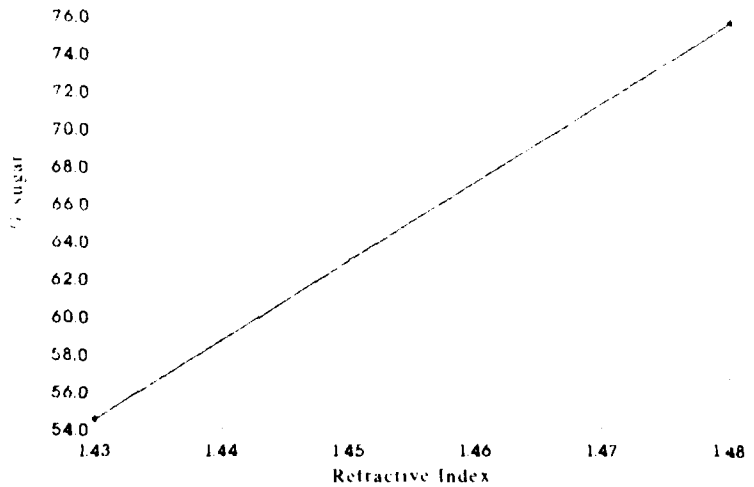

Figure 32: Calibration Curve for Refractometer

White light Source Faling Electro-optics. Tungsten halogen 100W lamp

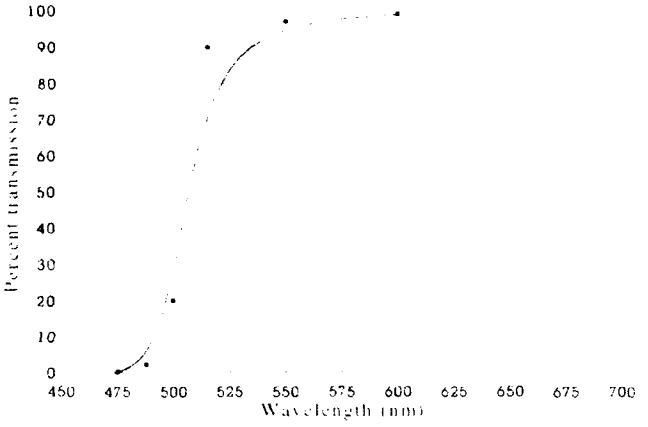

Figure 33: Calibration curve for OG515 filter

OG515 filter Melles-Griot.

ELECTRONIC

Lock-in Amplifier Model SR510 from Stanford Research Systems. Two input channels. External reference. Outputs include BNC, GPIB, RS232 interface

Power Meter Photon Control Surface Absorber, Model 25. Reflectivity constant two percent from 190nm to 22 microns.

Large area Photodiode RS Components (12508) $1cm^2$ active area. Peak response at 900 nm.

Motor Controller:

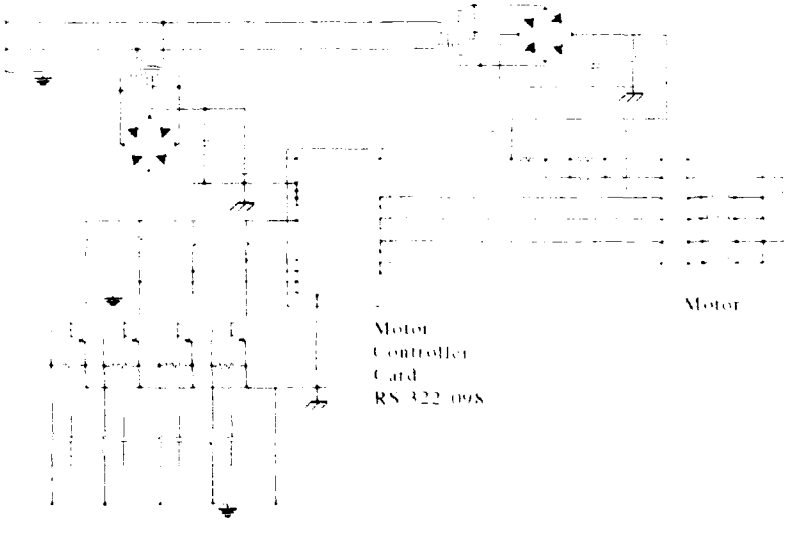

Figure 34: Motor Controller Circuit Diagram

Data Acquisition Card Model PCL-812PG enhanced multi-lab card.16 analog input channels, 16 digital output channels, and 16 digital input channels.

Computer Opus PC-V AT IBM-compatible. Monochrome monitor. Borland Pascal version 6.0 (analysis software).

CHEMICAL

pH Meter	RS 610-540. Measurement range 0-14 pH units, resolution .01 pH, repeatability +/- .02 pH, and accuracy +/- .03 pH.
Fluorescein	Uranin/Uranine/Disodium fluorescein/Yellow fluorescein/Fluorescein sodium. MW 376.28, $C_{20}H_{10}O_5Na_2$. Fisons Lab Reagent
Methanol	MW 32.04. CH_3OH. Reagent mixture. Fisons Specified Lab Reagent.
Dimethyl sulfoxide	MW 78.13. CH_3SOCH_3. Reagent grade BDH AnalaR
Acetic acid, glacial	MW 60.05. CH_3CO_2H. 17.4 M Reagent grade Aldrich.
Potassium Hydroxide	MW 56.11. KOH. 100 M (in water). Fisons Analytical Reagent.
Buffer Solutions	pH 4.0 (phthalate); actual value 4.01 at 20°C. pH 7.0 (phosphate); actual value 6.98 at 20°C pH 10.0 (borate); actual value 10.01 20°C. Fisons Analytical Supplies.

Appendix III
Characterisation of Some Evanescent Field Devices

In order to characterise some of the effects of elementary (non-tapered) evanescent field optical sensors, various researchers have invoked a bound ray analysis. This analysis describes the attenuation of the bound ray as it propagates. To fully describe the attenuation in the cladding, a wave effect is incorporated into the ray description. This analysis draws heavily on material absorption as described by Snyder and Love.

To describe the power of an evanescent wave, Snyder and Love introduce the power attenuation coefficient $\gamma(z)$ of a ray:

$$\gamma(z) = \frac{-1}{P(z)} \frac{dP(z)}{dz} \qquad \textit{Equation 3}$$

where $dP(z)$ is the the change in ray power due to the absorption in distance dz along the fibre. The fields associated with the local plane wave become evanescent and decrease exponentially with increasing distance from the axis. The evanescent fields lose some of their power to the absorbing cladding. The loss can be summed at N points in unit length of the fibre:

$$\gamma_{cl} = NT, \qquad \textit{Equation 4.1}$$

$$T = \frac{\text{power in reflected ray}}{\text{power in incident ray}} \qquad \textit{Equation 4.2}$$

The external media at the exposed portion of the core guides the field, and the power transmitted is

$$P(z) = P(0)\exp^{-\gamma z} \qquad \textit{Equation 5}$$

where z is the distance along the unclad length, $P(0)$ is power transmitted in the absence of an absorbing species. In the case of the single mode fibre,

$$P(z) = P(0)\exp^{-r\alpha z} \qquad \textit{Equation 6}$$

where α is the bulk absorbance coefficient of the external fluid. The overall evanescence absorbance for an unclad fibre of length L is

$$A = \frac{\gamma L}{2.303} = \frac{r\alpha L}{2.303} \qquad \textit{Equation 7}$$

where r is $\frac{4\sqrt{2}}{3V}$, fraction of power outside the core. [42]

The description of the field in tapered fibres is based on modal field analysis, using LP notation as appropriate for the fundamental (and all other l=0) modes.

Endnotes

1. Otto S. Wolfbeis, "Chemical sensors - surveys and trends," Fresenius' Journal of Analytical Chemistry 337 (1990): 523.

2. John O.W. Norris, "Current Status and Prospects for the Use of Optical Fibres in Chemical Analysis: A Review," Analyst 114 (November 1989): 1359.

3. Robert A. Lieberman, L.L. Blyler and Leonard G. Cohen, "A Distributed Fiber Optic Sensor Based on Cladding Fluorescence," Journal of Lightwave Technology 8 (February 1990):212.

4. Norris, 1363.

5. R.A. Lieberman, "Recent Progress in Intrinsic Fiber Optic Chemical Sensing," in Proceedings SPIE Vol. 1368: Chemical, Biochemical, and Environmental Fiber Sensors II, ed. RA Lieberman and MT Wlodarczyk, (Bellingham, WA, Society of Photo-Optical Instrumentation Engineers, 1990), 15.

6. Norris, 1367.

7. Norris, 1368.

8. Lieberman, "Recent Progress in Intrinsic Fiber Optic Chemical Sensing," 19.

9. Helmut Offenbacher, Otto S. Wolfbeis, and Eva Furlinger, "Fluorescence Optical Sensors for Continuous Determination of Near-Neutral pH Values," Sensors and Actuators 9 (1986): 77.

10. J.Y. Ding, M.R. Shahriari, and G.H. Sigel, Jun., "Fiber Optic pH Sensors Prepared by Sol-Gel Immobilisation Technique," Electronics Letters 27 (15 August 1991): 1561.

MT Wlodarczyk. (Bellingham, WA. Society of Photo-Optical Instrumentation Engineers, 1990), 38.

42. A.W. Snyder and John D. Love, Optical Waveguide Theory, (London: Chapman and Hall, 1991), 124-126.

11. R. Ulrich and H.P. Weber, "Solution-Deposited Thin Films as Passive and Active Light-Guides," Applied Optics 11 (February 1972): 1972.

12. K.T.V. Grattan, G.E. Badini, A.W. Palmer, and A.C.C. Tseung, "Use of Sol-Gel Techniques for Fibre-Optic Sensor Applications," Sensors and Actuators A 25-27 (1991): 483.

13. B.D. MacCraith, V. Ruddy, C. Potter, B. O'Kelly, and J.F. McGilp, "Optical Waveguide Sensor Using Evanescent Wave Excitation of Fluorescent Dye in Sol-Gel Glass," Electronics Letters 27 (4 July 1991): 1247.

14. MacCraith, 1248.

15. Ming-Ren S. Fuh, Lloyd W. Burgess, Tomas Hirschfeld, Gary D. Christian, and Francis Wang, "Single Fibre Optic fluorescence pH Probe," Analyst 112 (August 1987): 1159.

16. Ding, 1561.

17. Francesco Baldini, "Recent Progress in Fiber Optic pH Sensing," in Proceedings: SPIE Vol. 1368: Chemical, Biochemical, and Environmental Fiber Sensors II, ed. RA Lieberman and MT Wlodarczyk, (Bellingham, WA, Society of Photo-Optical Instrumentation Engineers, 1990), 184.

18. Baldini, 187.

19. Offenbacher, 74.

20. Norris, 1362.

21. Frank Kvasnik and Andrew D. McGrath, "Distributed Chemical Sensing Utilising Evanescent Wave Interactions," in Proceedings: SPIE Vol. 1172: Chemical,

Biochemical, and Environmental Fiber Sensors, ed. MT Wlodarczyk, (Bellingham, WA, Society of Photo-Optical Instrumentation Engineers, 1989), 76.

22. V. Ruddy, B.D. MacCraith, and J.A. Murphy, "Evanescent Wave Absorption Spectroscopy using Multimode Fibers," Journal of Applied Physics 67 (15 May 1990): 6070.

23. Lieberman, "A Distributed Fiber Optic Sensor Based on Cladding Fluorescence," 215.

24. Ibid., 218.

25. F.P. Payne and H.S. Mackenzie, "Novel Applications of Monomode Fibre Tapers," in SPIE Vol. 1504: Fiber-Optic Metrology and Standards 1991: Proceedings of the Conference in the Hague, Netherlands, ed. O.D. Soares (Bellingham, WA, Society of Photo-Optical Instrumentation Engineers, 1990), 15.

26. Ibid., 167.

27. H.S. Mackenzie and F.P. Payne, "Saturable Absorption in a Tapered Single-Mode Optical Fibre," Electronics Letters 26 (11 November 1990): 1744.

28. H.S. Mackenzie and F.P. Payne, "Evanescent Field Amplification in a Tapered Single-Mode Optical Fibre," Electronics Letters 26 (18 January 1990): 131.

29. Baldini, 184.

30. Ibid., 188.

31. Klaus Gollnick, Theodor Franken, Mohamed F.R. Fouda, Hanns R. Paur, and Stephen Held, "Merbromin (Mercurochrome) and Other Xanthene Dyes: Quantum Yields of Triplet Sensitizer Generation and Singlet Oxygen Formation in Alcoholic Solutions," Journal of Photochemistry and Photobiology, B: Biology 12 (1992):58.

32. Zhan-gong Zhao, Tao Shen and Hui-Jun Xu, "The Absorption and Structure of Fluorescein and its Ethyl Derivatives in Various Solutions," Spectrochimica Acta 45A (1989): 114.

33. Ibid, 1116.

34. R. Reisfeld, M. Eyal and R. Guishi, "Spectroscopic Behaviour of Fluorescein and its Di(Mercury Acetate) Adduct in Glasses," Chemical Physics Letters 138 (24 July 1987): 378.

35. Fuh, 1161.

36. S. Speiser and F.L. Chisena, "Optical Bistability in Fluorescein Dyes," Applied Physics B 45 (1988): 142.

37. Ieva R. Politzer, Kathleen T. Crago, Tony Hampton, Jocelyn Joseph, Joseph H. Boyer, and Mayur Shah, "Effect of ß-Cyclodextrin on the Fluorescence, Absorption and Lasing of Rhodium 6G, Rhodamine B and Fluorescein Disodium Salt in Aqueous Solutions," Chemical Physics Letters 159 (7 July 1989):260.

38. Robert C. Weast, ed., Chemical Rubber Company Handbook of Chemistry and Physics: 1977-1978, 58th Edition (Cleveland, OH: CRC Press, Inc, 1978), D-220.

39. Weast, D-244.

40. D. Ricard, Ph. Roussignol, and Chr. Flytzanis, "Surface-mediated enhancement of optical phase conjugation in metal colloids," Optics Letters 10 (October 1985): 511.

41. David Lipson, Kevin D. McLeaster, Brian Cohn, and Robert E. Fischer, "Drilled Optical Fibre Sensors: A Novel Single Fibre Sensor," in Proceedings SPIE Volume 1368: Chemical, Biochemical, and Environmental Fiber Sensors II, ed. RA Lieberman and